

## ORIGINAL ARTICLE

## Enhanced oncolytic potency of vesicular stomatitis virus through vector-mediated inhibition of NK and NKT cells

J Altomonte<sup>1,4,5</sup>, L Wu<sup>1,5</sup>, M Meseck<sup>1</sup>, L Chen<sup>1</sup>, O Ebert<sup>1,6</sup>, A Garcia-Sastre<sup>2</sup>, J Fallon<sup>3</sup>, J Mandeli<sup>4</sup> and SLC Woo<sup>1</sup>

<sup>1</sup>Department of Gene and Cell Medicine, Mount Sinai School of Medicine, New York, NY, USA; <sup>2</sup>Department of Microbiology, Mount Sinai School of Medicine, New York, NY, USA; <sup>3</sup>Department of Pathology, Mount Sinai School of Medicine, New York, NY, USA and <sup>4</sup>Department of Community and Preventive Medicine, Mount Sinai School of Medicine, New York, NY, USA

Recombinant oncolytic viruses represent a promising alternative option for the treatment of malignant cancers. We have reported earlier the safety and efficacy of recombinant vesicular stomatitis virus (VSV) vectors in a rat model of hepatocellular carcinoma (HCC). However, the full potential of VSV therapy is limited by a sudden decline in intratumoral virus replication observed early after viral administration, a phenomenon that coincides with an accumulation of inflammatory cells within infected lesions. To overcome the antiviral function of these cells, we present a recombinant virus, rVSV-UL141, which expresses a protein from human cytomegalovirus known to downregulate the natural killer (NK) cell-activating ligand CD155. The modified vector resulted in an inhibition of NK cell recruitment *in vitro*, as well as decreased intratumoral accumulations of NK and NKT cells *in vivo*. Administration of rVSV-UL141 through hepatic artery infusion in immune-competent Buffalo rats harboring orthotopic, multi-focal HCC lesions resulted in a one-log elevation of intratumoral virus replication over a control rVSV vector, which translated to enhance tumor necrosis and substantial prolongation of survival. Moreover, these results were achieved in the absence of apparent toxicities. The present study suggests the applicability of this strategy for the development of effective and safe oncolytic agents to treat multi-focal HCC, and potentially a multitude of other cancers, in the future.

*Cancer Gene Therapy* (2009) 16, 266–278; doi:10.1038/cgt.2008.74; published online 10 October 2008

**Keywords:** oncolytic virotherapy; HCC; inflammatory response; natural killer cells; recombinant VSV

## Introduction

Hepatocellular carcinoma (HCC) represents a major health concern throughout the world, accounting for over one million cases annually.<sup>1–3</sup> Although the incidence of HCC has more than doubled over the last two decades,<sup>4,5</sup> the emergence of innovative treatment options remains extremely limited. Currently, only a small percentage of patients are candidates for curative treatments, because of underlying liver disease, extent of metastasis and limited availability of livers for transplantation.<sup>6</sup> The remaining majority of patients is eligible only for palliative treatments that result in modest prolongation of survival.<sup>7,8</sup>

HCC is therefore an aggressive disease, characterized by poor prognosis and limited treatment options, highlighting the critical need for the development of novel and effective therapeutic agents.

Oncolytic viruses have gained recognition as attractive alternatives to conventional cancer therapy, because of their intrinsic ability to selectively replicate and kill tumor cells *in vitro* and *in vivo*.<sup>9–12</sup> Vesicular stomatitis virus (VSV), a member of the Rhabdoviridae family, is a particularly appealing oncolytic vector because of its short replication cycle and ability to reach high titers in many rodent and human tumor cell lines. It is an enveloped, negative-strand RNA virus with a wide host range, which replicates selectively within tumor cells because of defects in antiviral type I interferon responses in these cells.<sup>13</sup> Although the natural hosts for VSV infection are cattle, horses and pigs, infections in humans are generally asymptomatic or result in mild febrile illness,<sup>14</sup> indicating that it has potential for safe clinical application in the future. Moreover, VSV is not endemic to the North American population, implying that there will not be preexisting neutralizing antibodies or memory cellular immune responses to interfere with its replication potential in patients.<sup>15</sup>

Correspondence: Professor SLC Woo, Department of Gene and Cell Medicine, Mount Sinai School of Medicine, One Gustave L. Levy Place, Box 1496, New York, NY 10029-6574, USA.

E-mail: savio.woo@mssm.edu

<sup>5</sup>These two authors contributed equally to this work.

<sup>6</sup>Current address: II. Medical Department, Klinikum rechts der Isar, Technical University of Munich, Munich, Germany

Received 13 April 2008; revised 3 July 2008; accepted 31 July 2008; published online 10 October 2008

We have described earlier the efficacy of recombinant VSV as an oncolytic vector for the treatment of orthotopic HCC in immune-competent rats.<sup>16</sup> We demonstrated that VSV, when administered at its maximum tolerated dose through the hepatic artery, could gain access to and selectively replicate in multi-focal HCC tumors of various sizes, resulting in tumor necrosis and prolongation of animal survival.<sup>17–19</sup> Although encouraging, complete tumor regression was not achieved, and the remaining viable tumor ultimately relapsed, resulting in the eventual demise of the treated animals. These observations encouraged us to seek an alternate approach to improve the outcome of VSV treatment for multi-focal HCC.

Following intra-arterial infusion of the vector, robust virus replication quickly commences within infected tumor cells, reaching a peak in viral titer at approximately 24 h post-treatment, followed by a logarithmic decline in subsequent days.<sup>17</sup> Given that the neutralizing antiviral antibody response in the host is not observed until later time points,<sup>17</sup> we suspected that the rapid reduction in intratumoral virus titers after the first day is instead the result of antiviral inflammatory responses launched at the site of infected tumor cells. Rapid recruitment and activation of cellular components of the innate immune system, such as granulocytes, natural killer (NK) cells, NKT cells and macrophages, have been observed at the sites of viral infection.<sup>20</sup> These cells participate in the antiviral response both by direct killing of infected cells and by production of antiviral cytokines. It was recently demonstrated that the host inflammatory response is correlated with the limited ability of herpes simplex virus (HSV) to replicate within tumor cells,<sup>21</sup> and suppression of inflammatory responses by treatment with chemotherapeutic cyclophosphamide resulted in enhanced anti-tumor efficacy of HSV.<sup>22</sup> On the basis of these data, coupled with our own observations of NK and NKT cell accumulation coinciding with the logarithmic decline of intratumoral VSV titers after 1 day, we demonstrated in a previous report that the host inflammatory response to VSV infection plays a critical role in the suppression of intratumoral VSV replication, and counteracting these responses substantially enhances VSV oncolysis and treatment efficacy.<sup>23</sup>

As the inflammatory processes of the host provide a difficult challenge to the survival of invading viruses, successful viral propagation within mammalian hosts is dependent, in part, on their ability to evade the antiviral arsenal launched by the host immune system. To this end, many viruses have evolved intricate mechanisms to evade detection and subsequent destruction by various immune cells in the host.<sup>24</sup> We have reported earlier a recombinant VSV vector, which encodes a viral chemokine-binding protein (vCKBP) derived from a heterologous virus, for the purpose of inhibiting antiviral inflammatory cells *in vivo*. In that study, we characterized a vector expressing the secreted form of the equine herpesvirus-1 glycoprotein G (gG<sub>EHV-1</sub>), which is a known vCKBP, and demonstrated that the expression of gG<sub>EHV-1</sub> inhibited the accumulation of NK and NKT cells within treated

tumors, which resulted in an improvement in therapeutic outcome. However, given that gG<sub>EHV-1</sub> is considered to be a broad-range vCKBP, which binds C, CC, and CXC chemokines with high affinity,<sup>25</sup> in our current study, we sought to employ an alternate strategy to further substantiate our hypothesis, while simultaneously restricting the specificity of the transgene to NK and NKT cells.

Here, we present a novel VSV vector, rVSV-UL141, which expresses a gene cloned from human cytomegalovirus (HCMV), known to inhibit the function of NK cells by blocking the ligand of NK cell-activating receptors. In addition to the inhibitory function on NK cells, we demonstrated that UL141 also blocks the migration of NKT cells to infected tumor sites, and the combined effect resulted in greatly elevated intratumoral virus replication, leading to enhanced tumor necrosis and substantially prolonged survival of immune-competent rats bearing syngeneic and multi-focal HCC lesions in the liver.

## Materials and methods

### Cell lines

The rat HCC cell line McA-RH7777 was purchased from the American Type Culture Collection (ATCC) (Manassas, VA) and maintained in Dulbecco's Modified Eagle's Medium (DMEM) (Mediatech, Herndon, VA) in a humidified atmosphere at 10% CO<sub>2</sub> and 37 °C. BHK-21 cells (ATCC) were maintained in DMEM in a humidified atmosphere at 5% CO<sub>2</sub> and 37 °C. All culture media were supplemented with 10% heat-inactivated fetal bovine serum (Sigma-Aldrich, St Louis, MO, USA) and 100 U ml<sup>-1</sup> penicillin–100 mg ml<sup>-1</sup> streptomycin (Mediatech).

### Plasmid construction

The construction of the recombinant VSV vector expressing mutant (L289A) Newcastle Disease Virus fusion protein (rVSV-F) was described earlier.<sup>18</sup> To clone a secreted form of the UL141<sub>HCMV</sub> gene, the predicted C-terminal transmembrane domain was determined by hydrophobicity plot to correspond to the first 823 bp of the UL141 open reading frame, which was consistent with the findings of others.<sup>26</sup> This portion of the UL141 open reading frame, with a stop codon and appropriate restriction sites for subsequent cloning, was synthesized chemically (GenScript, Piscataway, NJ). To generate a VSV plasmid simultaneously expressing UL141<sub>HCMV</sub> and firefly luciferase, the ubiquitously expressed encephalomyocarditis virus (ECMV) internal ribosomal entry site was introduced such that the two genes could be co-translated as a single transcriptional unit. This cassette was inserted into the full-length pVSV-XN2 plasmid, using the unique restriction sites *XhoI* and *NheI* in the untranslated region of the endogenous VSV glycoprotein. This was the same cloning scheme employed in the construction of rVSV-gG<sub>EHV-1</sub> described in our earlier publication.<sup>23</sup> Sequencing of the plasmids was conducted in the DNA Sequencing Core Facility at Mount Sinai School of Medicine.

### Generation of recombinant viruses

To rescue the recombinant VSV vectors, an established method of reverse genetics was employed.<sup>27,28</sup> Briefly, BHK-21 cells were infected with vaccinia virus expressing the T7 RNA polymerase (vTF-7.3), and subsequently transfected with the full-length rVSV plasmid in addition to plasmids encoding VSV N, P and L proteins using LipofectAMINE 2000 transfection reagent (Invitrogen, Carlsbad, CA). At 72 h post-transfection, supernatants were centrifuged and filtered through a 0.22  $\mu\text{m}$  filter to remove the majority of vaccinia virus, and transferred onto fresh BHK-21 cells. Any remaining vaccinia virus was eliminated by plaque purification, and the titers of recombinant VSV stocks were determined by plaque assays on BHK-21 cells.

### Multicycle growth curves

Morris (McA-RH7777) cells were plated in 24-well plates at  $5 \times 10^4$  cells per well and infected at a multiplicity of infection (MOI) of 0.01 with rVSV-F or rVSV-UL141 in triplicate. After infection at room temperature for 30 min, cells were washed twice with phosphate-buffered saline (PBS) to remove any unabsorbed virus, and fresh complete medium was added. At the indicated time points after infection, 100  $\mu\text{l}$  of supernatant was collected and assayed for viral titer by tissue culture infectious dose (TCID)<sub>50</sub> assays.

### In vitro cytotoxicity assay

McA-RH7777 cells were seeded in 24-well plates at  $5 \times 10^4$  cells per well overnight and then infected with rVSV-F or rVSV-UL141 in triplicate, at an MOI of 0.01 the following day. Cell viability was measured at the indicated time points after infection using the 3-(4,5-dimethylthiazol-2-yl)-2,5-diphenyltetrazolium bromide (MTT) assay (Cell Proliferation Kit I; Roche, Indianapolis, IN). All cell viability data are expressed as a percentage of viable cells as compared with mock-infected controls at each time point.

### In vitro NK cell migration assay

For preparation of rat NK cells, spleens were harvested from male Buffalo rats 24 h following treatment with 10  $\mu\text{g g}^{-1}$  of Poly I:C (EMD Biosciences, La Jolla, CA) by i.p. injection. The mononuclear cells in splenocytes were dispersed from the spleens, followed by gradient centrifugation in Lympholyte Cell Separation Media (Cedarlane, Ontario, Canada). NK cells were enriched from the mononuclear cells by Miltenyi magnetic separation after binding the cells with phycoerythrin (PE)-conjugated anti-rat CD161 $\alpha$  antibody (BD Biosciences, San Diego, CA), followed by anti-PE MicroBeads (Miltenyi Biotec, Auburn, CA), according to the manufacturer's instructions. Analysis by flow cytometry revealed that the preparations were >85% pure. The purified cells were cultured in complete DMEM medium containing 0.5% bovine serum albumin (Sigma-Aldrich). To determine the optimal concentration of rat macrophage inflammatory protein-1 $\alpha$  (MIP-1 $\alpha$ ) for the migration of rat NK cells, a dose-response study was conducted in 24-well transwell plates

(Corning INC, Corning, NY) with 5  $\mu\text{m}$  pore size filters using 0, 25, 50, 100 or 200  $\text{ng ml}^{-1}$  of rat MIP-1 $\alpha$  (Peprotech, Rocky Hill, NJ) in the lower chambers followed by a 4 h incubation at 37  $^{\circ}\text{C}$ . Migration of rat NK cells ( $5 \times 10^5$  per well) from the upper to lower chamber in response to the varying concentrations of chemokine was monitored. McA-RH7777 cells in serum-free DMEM (Mediatech) were infected with rVSV-F or rVSV-UL141 at an MOI of 5. The culture media were harvested 24 h post-infection, and filtered through 0.2  $\mu\text{m}$  Acrodisc syringe filters (Pall Corp., Ann Arbor, MI) after infectious virus in the filtrate was quantitatively inactivated by UV irradiation. At the defined dose of 100  $\text{ng ml}^{-1}$  of MIP-1 $\alpha$ , migration of rat NK cells was measured in the presence of the filtered and UV-inactivated culture supernatants.

### Animal studies

All procedures involving animals were approved and performed according to the guidelines of the Institutional Animal Care and Use Committee of the Mount Sinai School of Medicine. Male Buffalo rats (5–7 week old) weighing 200 g were purchased from Charles River Labs (Wilmington, MA) and housed in a specific pathogen-free environment under standard conditions. To establish multi-focal HCC lesions within the liver, 10<sup>7</sup> syngeneic McA-RH7777 rat HCC cells were infused into the portal vein in a 1 ml suspension in serum-free DMEM. At 21 days after tumor cell implantation, the development of multi-focal hepatic tumors of 1–10 mm in diameter was confirmed, and  $1 \times 10^7$  plaque-forming units (p.f.u.) of rVSV-UL141 or rVSV-F or PBS control (in 1 ml total volume) were administered through the hepatic artery. To evaluate tumor response to treatment, animals were killed 3 days after infusion and tumors were subjected to histological, immunohistochemical and immunofluorescent staining, as well as TCID<sub>50</sub> analysis of tumor extracts for quantification of VSV yield. In addition, groups of animals infused with VSV vectors or PBS were followed for survival, which was monitored daily in all animals.

### Histology and immunohistochemistry

Liver sections containing tumor were fixed overnight in 4% paraformaldehyde and then paraffin-embedded. Here, 5- $\mu\text{m}$ -thin sections were subjected to either hematoxylin and eosin staining for histological analysis or immunohistochemical staining using monoclonal antibodies against VSV-G protein (Alpha Diagnostic, San Antonio, TX), myeloperoxidase (MPO) (Abcam, Cambridge, MA). A second set of liver sections containing tumor were fixed overnight in 4% paraformaldehyde and then equilibrated in 20% sucrose in PBS overnight. Here, 5- $\mu\text{m}$ -thin frozen sections were subjected to immunohistochemical staining using monoclonal antibodies against NKR-P1A (BD Pharmingen, CA), OX-52 (BD Pharmingen, San Jose, CA), or ED-1 (Chemicon, Billerica, MA). Semiquantification of positively stained cells was performed using ImagePro Software (Media Cybernetics Inc., Silver Spring, MD), and immune cell

index was calculated as a ratio of positive cell number to unit tumor area (10 000 pixels as one unit tumor area).

*Indirect immunofluorescence*

Tumor-containing liver samples were obtained on day 3 after virus or PBS infusion. Here, 5 μm-thin frozen sections were fixed with cold acetone and blocked with 4% goat serum, followed by staining with R-PE-conjugated mouse anti-rat CD3 monoclonal antibody (BD Pharmingen) and fluorescein isothiocyanate-conjugated mouse anti-rat NKR-P1A antibody (BD Pharmingen). Nuclear DNA was stained with 4',6'-diamidino-2-phenylindole. Cover slips were mounted on glass slides using VECTASHIELD Mounting Medium (Vector Laboratories, Burlingame, CA).

*Statistical analyses*

For comparison of individual data points, two-sided Student's *t*-test was applied to determine statistical significance. Survival curves of animals were plotted according to the Kaplan–Meier method, and statistical significance in different treatment groups was compared using the log-rank test. Results and graphs were obtained using the GraphPad Prism 3.0 program (GraphPad Software, San Diego, CA).

**Results**

*Functional characterization of a recombinant VSV vector expressing the UL141 gene from HCMV*

After rescue of the recombinant rVSV-UL141 vector, through the established reverse genetics system described earlier,<sup>27,28</sup> the vector was subjected to various methods of

characterization. We have shown earlier that the recombinant vector rVSV-F, which expresses a genetically modified NDV fusion membrane glycoprotein, replicated to similar titers as wild-type VSV in BHK-21 and hepatoma cells.<sup>18</sup> To determine whether or not the expression of the UL141 transgene altered the infectivity or replication of the virus, growth curves of rVSV-UL141 were compared with that of rVSV-F *in vitro*. TCID<sub>50</sub> assays were performed from supernatants collected at various time points after infection of the rat HCC cell line McA-RH7777 with each virus at an MOI of 0.01 (Figure 1a). At each time point, the vectors replicated to similar titers, indicating that the inclusion of the UL141 gene in the recombinant vector did not significantly alter the viral life cycle or viral yield of VSV in rat HCC cells *in vitro*.

To compare the tumor cell-killing potential of the VSV vectors *in vitro*, McA-RH7777 cells were infected with either rVSV-UL141 or rVSV-F at an MOI of 0.01, or mock-infected. The cytotoxicity to the cells was quantified by MTT assay, and calculated as a percentage of mock-infected cells at each time point. Although there appeared to be an initial delay in the cell-killing effects observed in rVSV-UL141-infected cells as compared with rVSV-F, the kinetics were not significantly different, and by 48 h post-infection both viruses resulted in nearly 100% cell death (Figure 1b), demonstrating that rVSV-UL141 is an effective oncolytic agent in Morris hepatoma cells *in vitro*.

*In vitro inhibition of NK cell migration by conditioned media from rVSV-UL141-infected rat HCC cells*

To determine whether the UL141<sub>HCMV</sub> protein expressed by rVSV-UL141-infected cells is functional, assays to look at the migration of NK cells in response to MIP-1α were

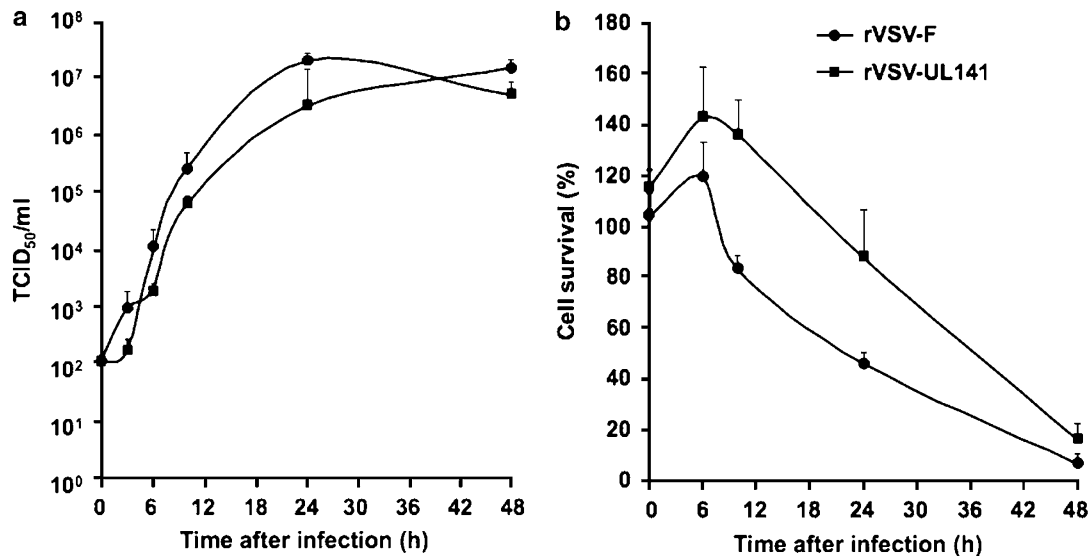


**Figure 1** Viral replication and cell killing by rVSV-UL141 versus rVSV-F in Morris (McA-RH7777) rat hepatoma cells *in vitro*. Rat hepatoma cells were infected with rVSV-F or rVSV-UL141 at a multiplicity of infection (MOI) of 0.01. (a) TCID<sub>50</sub> assay was performed on conditioned media at 0, 3, 6, 10, 24 and 48 h post-infection; (b) 3-(4,5-di0methylthiazol-2-yl)-2,5-diphenyltetrazolium bromide (MTT) assays for cell viability were performed at 0, 3, 6, 10, 24 and 48 h post-infection. Triplicate samples were analyzed at each time point. Data are shown as mean ± standard deviation.

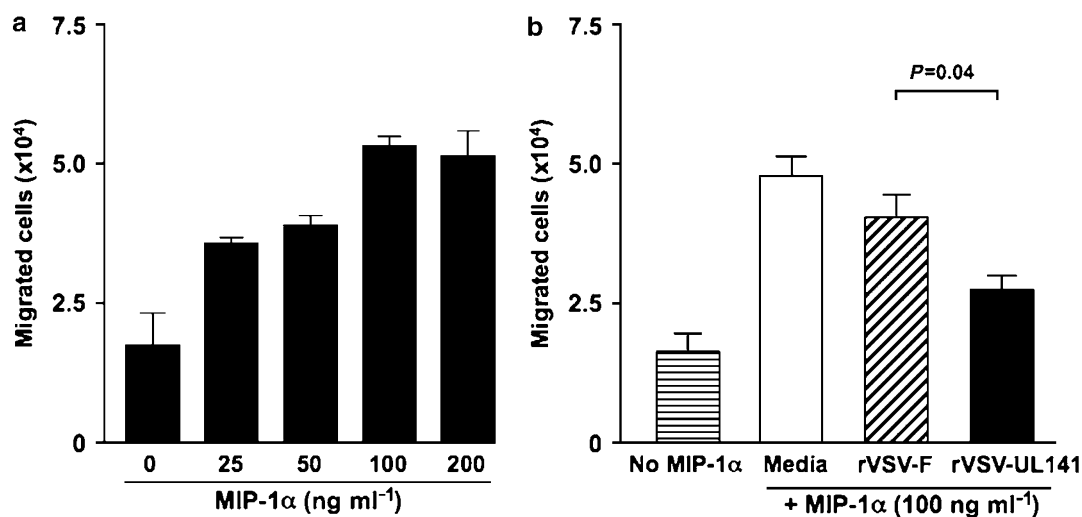


**Figure 2** Inhibition of natural killer (NK) cell migration by conditioned media from rVSV-UL141-, but not rVSV-F-, infected rat hepatocellular carcinoma (HCC) cells. **(a)** Dose–response of rat NK cell migration in response to rat macrophage inflammatory protein-1 $\alpha$  (MIP-1 $\alpha$ ). The migration assays were performed using 24-well transwell plates. The migration of rat NK cells from the upper chamber to the lower chamber in response to serially diluted rat MIP-1 $\alpha$  (0–200 ng ml<sup>-1</sup>) was monitored. **(b)** Inhibition of NK cell migration in response to MIP-1 $\alpha$  by conditioned media from rVSV-infected rat HCC cells. The migration assays were performed using 24-well transwell plates. The migration of rat NK cells from the upper chamber to the lower chamber in response to 100 ng ml<sup>-1</sup> of MIP-1 $\alpha$  was monitored in the presence of ultrafiltered and UV-inactivated supernatants from 10<sup>5</sup> HCC cells infected with rVSV-UL141 or rVSV-F. Data presented are the mean values of four independent experiments and the results were analyzed statistically by two-sided Student's *t*-test.

performed in 24-well transwell plates. To define the optimal dose of rat MIP-1 $\alpha$  in the lower chamber for the recruitment of rat NK cells, a dose–response experiment was performed using increasing concentrations of MIP-1 $\alpha$ , whereas the number of rat NK cells added to the upper chamber remained constant. The migration of NK cells from the upper to the lower chamber was monitored, and it was determined that NK cell migration increased in an MIP-1 $\alpha$  dose-responsive manner until saturation was reached at 100 ng ml<sup>-1</sup> (Figure 2a). This dose of MIP-1 $\alpha$  was then used in subsequent experiments to evaluate the inhibition of rat NK cell migration by conditioned media from rVSV-UL141- versus rVSV-F-infected rat McA-RH7777 hepatoma cells, which were ultrafiltered and UV-irradiated to quantitatively remove infectious viruses. As controls, media from mock-infected cells and migration in the absence of MIP-1 $\alpha$  were used. The results showed that the number of migrating NK cells was significantly inhibited by conditioned media from rVSV-UL141-infected rat HCC cells as compared with that from rVSV-F- and mock-infected cells (Figure 2b; *P* = 0.01).

#### Enhanced replication of rVSV-UL141 in orthotopic, multi-focal HCC tumors in syngeneic and immune-competent rats

To assess the *in vivo* effect of vector-mediated intratumoral UL141 production on oncolysis and viral replication within tumors, multi-focal HCC lesions were produced through injection of McA-RH7777 cells through the portal vein of male Buffalo rats as described earlier.<sup>17</sup> At 21 days post-implantation, the presence of multi-focal HCC lesions ranging from 1 to 10 mm in diameter was confirmed by laparotomy, and these

animals were treated with PBS or 1  $\times$  10<sup>7</sup> p.f.u. of rVSV-UL141 or rVSV-F through hepatic artery infusion. Animals from each group were killed on day 3 after treatment, and tumor samples were collected and fixed for histological and immunohistochemical staining, as well as snap-frozen for intratumoral viral titer quantification. Immunohistochemical staining using a monoclonal antibody against VSV-G revealed significantly more abundant expression of VSV-G protein within the tumors of rVSV-UL141-treated animals, as compared with that observed in the rVSV-F group (Figure 3A). To quantify the virus titers within the lesions, lysates prepared from snap-frozen tumor samples from each animal were subjected to TCID<sub>50</sub> analysis. Although rVSV-F infusion resulted in titers less than 10<sup>4</sup> TCID<sub>50</sub> per mg of tumor tissue, rVSV-UL141 replicated to yield titers of one-log higher at almost 10<sup>5</sup> TCID<sub>50</sub> per mg of tumor tissue (Figure 3B; *P* = 0.04).

#### Improved tumor response in multi-focal HCC lesions in the livers of rats treated with rVSV-UL141

To determine the impact of enhanced intratumoral replication of the rVSV-UL141 vector on tumor viability, tumor-containing liver sections from the above experiment were examined by hematoxylin and eosin staining and analyzed morphometrically for quantification of necrotic area (Figure 4A). Using ImagePro analysis software, necrotic areas were measured and represented as a percentage of the entire tumor area. Tumors within the rVSV-UL141 treatment group were more than 50% necrotic, which represents a significant increase over the rVSV-F treatment group, which exhibited approximately 25% necrosis (Figure 4B; *P* = 0.01). In the PBS control

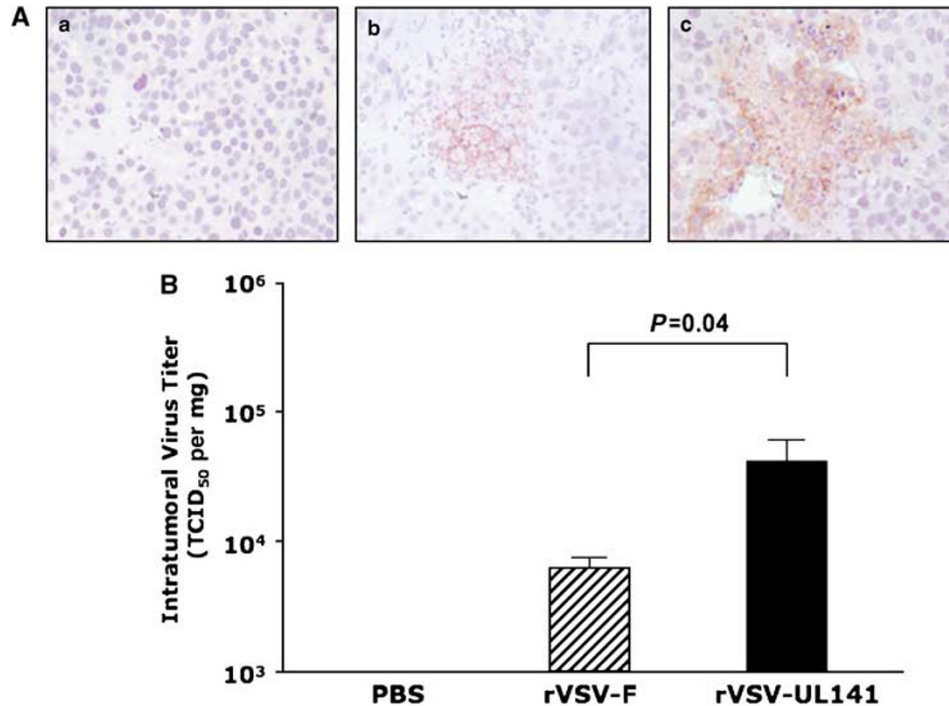


**Figure 3** rVSV-UL141 versus rVSV-F replication in hepatocellular carcinoma (HCC) tumors in the livers of immune-competent Buffalo rats. Multi-focal HCC-bearing Buffalo rats were treated with phosphate-buffered saline (PBS) ( $n=3$ ), rVSV-F ( $n=4$ ) or rVSV-UL141 ( $n=4$ ) at  $1 \times 10^7$  p.f.u. per rat injected through the hepatic artery. Tumor samples were obtained from the treated rats at day 3 after virus infusion. Here, 5- $\mu$ m tumor sections were stained with a monoclonal anti-VSV-G antibody and counterstained with hematoxylin and eosin (A). Representative sections from rats treated with PBS, rVSV-F and rVSV-UL141 are shown in (a–c), respectively (magnification =  $\times 40$ ). In (B), intratumoral virus titers were determined by TCID<sub>50</sub> assays performed using tumor extracts on BHK-21 cells. Viral titers are expressed as TCID<sub>50</sub> per mg tissue (mean  $\pm$  standard deviation), and the results were analyzed statistically by two-sided Student's *t*-test.

group, less than 15% necrosis was observed, which can be attributed to spontaneous necrosis that is a natural phenomenon in this tumor type *in vivo*.

Because this treatment strategy employs a transgene designed to inhibit a key component of the antiviral inflammatory response in the host, safety was an obvious concern. To identify signs of hepatic toxicity, histopathological sections showing the border region between tumor and liver tissues and neighboring liver parenchyma were examined. It was determined that the surrounding liver histology was completely normal, with no evidence of abnormal pathology (results not shown).

#### Decreased accumulation of NK and NKT cells in tumors treated with rVSV-UL141 as compared with rVSV-F

Multi-focal HCC tumor-bearing Buffalo rats were treated with either PBS or  $1 \times 10^7$  p.f.u. of rVSV-UL141 or rVSV-F through the hepatic artery. On day 3 after treatment, animals were killed, and tumor-containing liver sections were prepared for immunohistochemical staining of various immune cell types (Figure 5A). Sections were stained for NK cells with anti-NKR-P1A (frames a–c), neutrophils by anti-myeloperoxidase (frames d–f), pan-T cells by anti-OX-52 (frames g–i) and macrophages by anti-ED-1 (frames j–l). Semiquantification of marker-positive cells using ImagePro software revealed that there was substantial intratumoral accumulation of NK cells after rVSV-F infusion as compared with PBS (Figure 5Ba;

$P=0.04$ ); however, this effect was substantially reduced in response to rVSV-UL141 treatment (Figure 5Ba;  $P=0.002$ ). In addition, there were significantly fewer pan-T marker-positive cells (Figure 5Bc;  $P=0.04$ ) in tumors treated with rVSV-UL141 as compared with those treated with rVSV-F. There were no difference in PBS, rVSV-F, rVSV-UL141 groups (Figure 5Bb, 5Bd). To determine whether these were NKT cells or T-lymphocytes, indirect immunofluorescent staining was performed. Consecutive tumor sections from PBS-, rVSV-UL141- or rVSV-F-treated animals were stained with R-PE-conjugated mouse anti-rat CD3 antibody and fluorescein isothiocyanate-conjugated mouse anti-rat NKR-P1A antibody (Figure 6). Merged images indicate that the pan-T-positive cells present in the tumors after rVSV-F treatment are in fact NKT cells rather than T-lymphocytes. As expected, there were no statistically significant differences in neutrophil ( $P=0.6$ ) or macrophage accumulation ( $P=0.08$ ) within tumors of rats treated with the two rVSV vectors. Collectively, these results indicate that the inhibitory function of UL141 on inflammatory cells is specific for NK and NKT cells.

#### Substantial prolongation of survival of multi-focal HCC-bearing rats treated with rVSV-UL141 versus rVSV-F

To assess the oncolytic potential of a rVSV vector expressing a transgene that inhibits NK and NKT cell function, rats bearing orthotopic multi-focal HCC tumors

were randomly assigned to treatment groups to receive PBS ( $n=8$ ) or  $1 \times 10^7$  p.f.u. of rVSV-UL141 ( $n=14$ ) or an equal dose of the control rVSV-F vector ( $n=10$ ). All animals received a single infusion of the respective treatment through the hepatic artery, and animals were monitored daily for survival (Figure 7). In addition, all animals were carefully screened for clinical signs of treatment-associated toxicity to address safety concerns of the modified virus. Although all animals in the PBS or rVSV-F treatment groups expired by day 21 or 29, respectively, rVSV-UL141 treatment resulted in a highly significant prolongation of survival ( $P<0.001$ ), with 3 out of 14 animals (21.4%) achieving long-term survival of 150 days. Furthermore, the long-term surviving rats in the rVSV-UL141 treatment group were killed on day 150 and evaluated for residual malignancy. Macroscopically, there was no visible tumor within the liver or elsewhere, and there was no histological evidence of residual tumor cells or hepatitis. These results indicate that even large multi-focal lesions (up to 10 mm in diameter at the time of treatment) had undergone complete

remission in these animals, which translated into long-term and tumor-free survival.

## Discussion

Various strategies have been explored to enhance the oncolytic potency of recombinant VSV vectors, with the aim of improving the therapeutic potential of the virus. In the present study, we have presented a novel rVSV vector that encodes a heterologous viral protein, which specifically inhibits the function of NK cells. We developed this vector as an effective yet safe oncolytic agent for the treatment of multi-focal HCC in an immune-competent rat model. The data presented here support our hypothesis that by inhibition of a specific aspect of the host inflammatory response, we can greatly enhance the oncolytic potency over the rVSV-F construct, without compromising the safety profile. This strategy translates into highly significant prolongation of survival with 20%

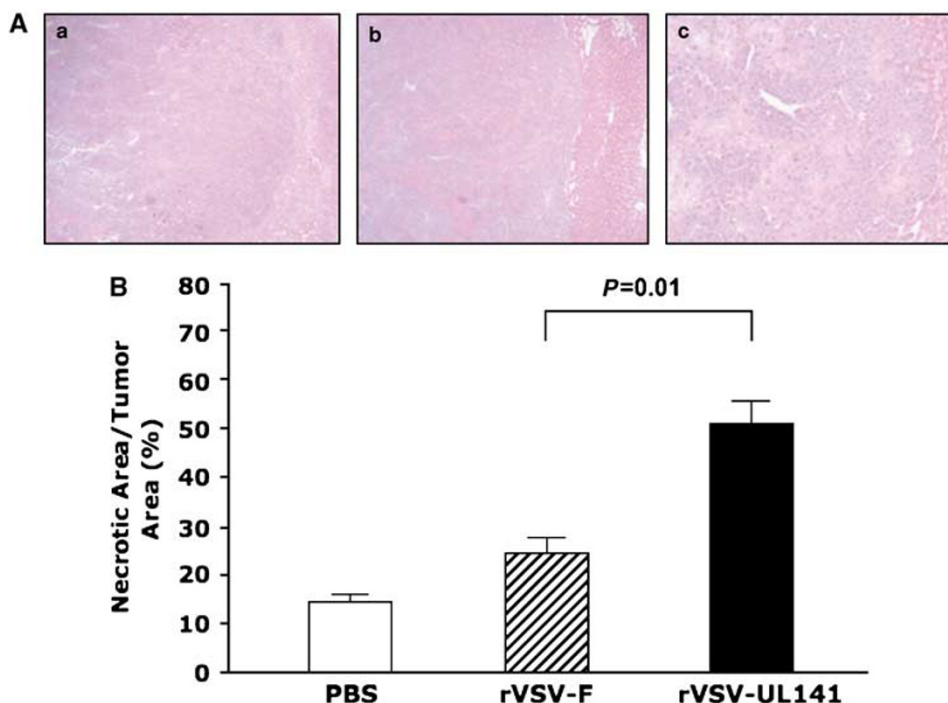
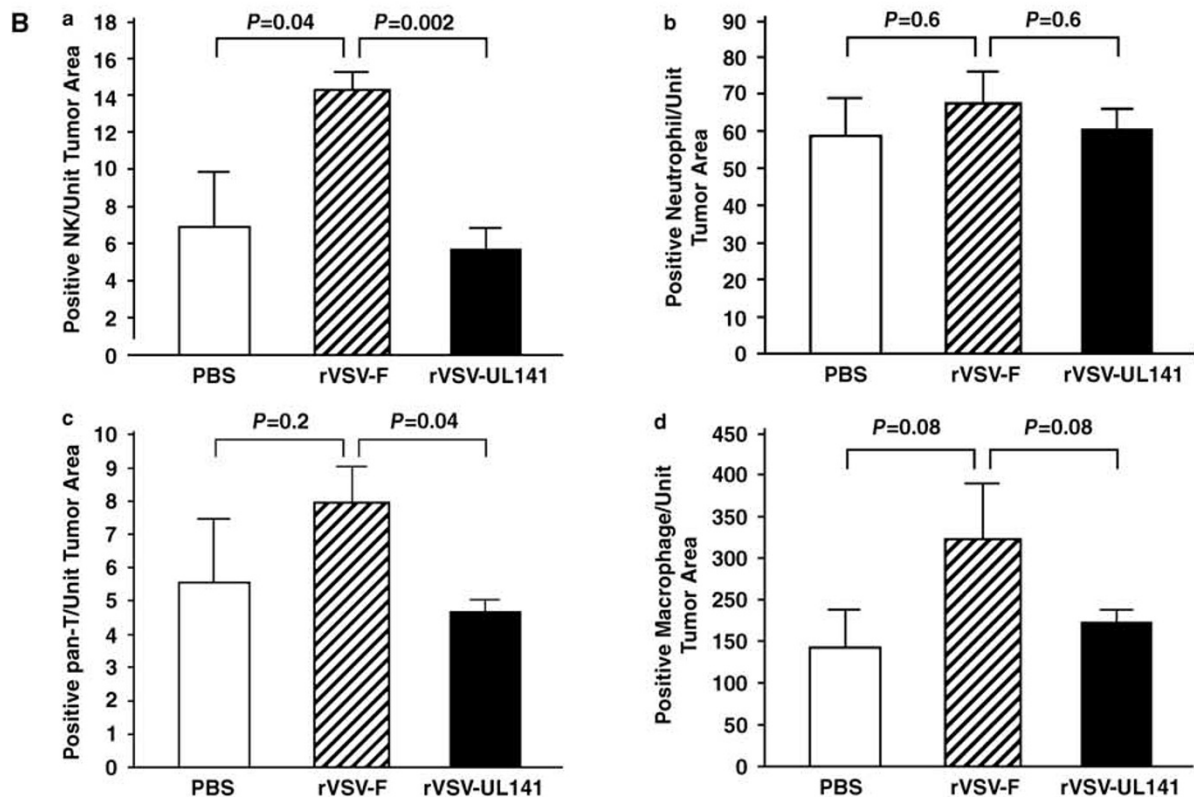
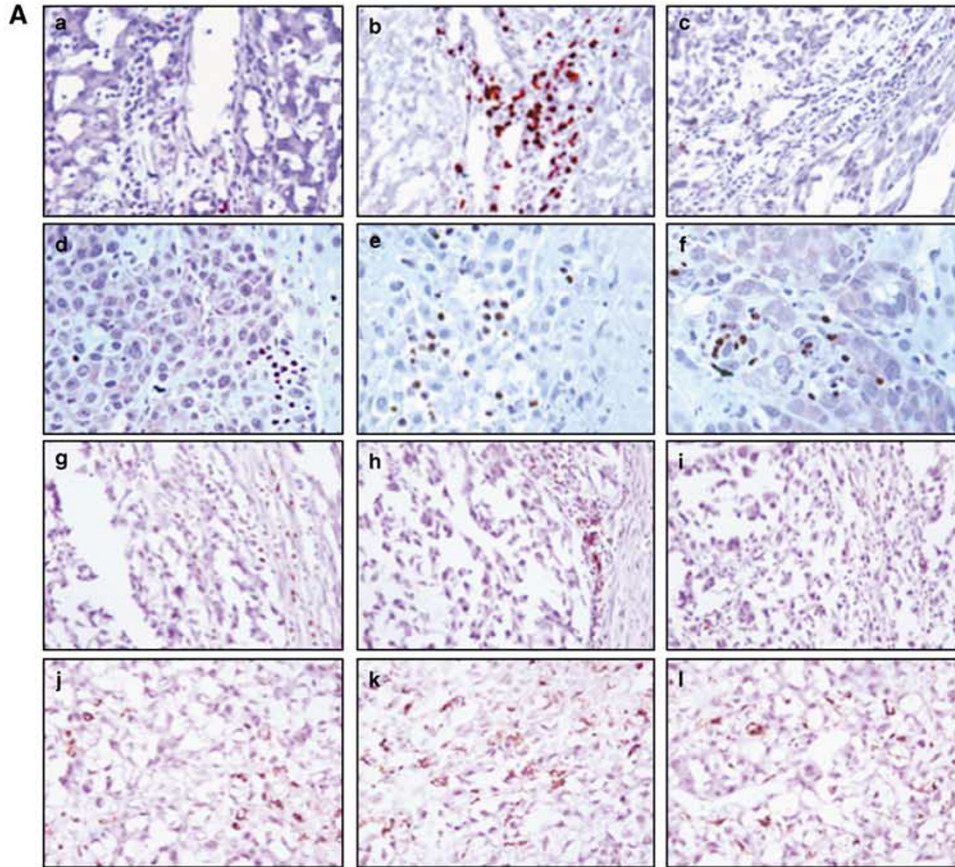


**Figure 4** Enhanced tumor response in rats treated with rVSV-UL141 versus those treated with rVSV-F. Multi-focal hepatocellular carcinoma (HCC)-bearing Buffalo rats were injected through the hepatic artery with phosphate-buffered saline (PBS) ( $n=3$ ), rVSV-F ( $n=4$ ) or rVSV-UL141 ( $n=4$ ) at  $1 \times 10^7$  p.f.u. per rat and killed 3 days post-treatment. (A) Here, 5- $\mu$ m tumor sections were stained with hematoxylin and eosin (H&E). Representative sections from rats treated with PBS, rVSV-F and rVSV-UL141 are shown in (a–c), respectively (magnification =  $\times 40$ ). (B) Percentage of necrotic areas in the tumors were measured morphometrically using ImagePro software. Data are shown as mean  $\pm$  standard deviation, and the results were analyzed statistically by two-sided Student's *t*-test.

**Figure 5** Immunohistochemical staining and semiquantification of immune cells in tumors. (A) Representative immunohistochemical sections from tumors and surrounding tissues. Tumor-bearing rats were infused with phosphate-buffered saline (PBS) (a, d, g, j), rVSV-F (b, e, h, k) or rVSV-UL141 (c, f, i, l) at  $1 \times 10^7$  p.f.u. ml<sup>-1</sup> per rat. Samples were obtained from rats at day 3 after virus infusion into the hepatic artery. Here, 5- $\mu$ m sections were stained with mouse monoclonal anti-NKR-P1A (a–c), polyclonal anti-myeloperoxidase (d–f), monoclonal anti-OX-52 (g–i) and monoclonal anti-ED-1 (j–l), (magnification =  $\times 40$ ). (B) Semiquantification of immune cells in the lesions after virus treatment: NK cells (a), neutrophils (b), pan-T cells (c) and macrophages (d) by ImagePro software. Immune cell index was calculated as a ratio of positive cell to unit tumor area (10000 pixel as one unit tumor area), and the results were analyzed statistically by two-sided Student's *t*-test.



of treated animals enjoying complete tumor regression and long-term survival, whereas all rVSV-F-treated animals succumbed to the disease by day 30 post-treatment. Furthermore, these results were achieved after a single administration of the vector.

It is important to note that rVSV-F, and not wtVSV, was used as a control vector in these studies. It is our strategy when testing new recombinant vectors, we compare them with our currently best available vector. In this way, we can directly assess whether or not the new vector represents an improvement over our prior work. Because we had reported earlier a significant improvement in the efficacy of the fusogenic rVSV-F vector over the wild-type version,<sup>18,29</sup> it seemed intuitive to use this vector as a control for comparison of the rVSV-UL141 vector.

We have recently shown that vector-mediated suppression of antiviral inflammatory responses is a novel and effective strategy for enhancing the potency of VSV for the treatment of multi-focal HCC in rats. We hypothesized that the logarithmic decline in intratumoral virus replication observed at an early phase of infection was mediated by antiviral inflammation, which was evident within the lesions after 1–2 days. This was confirmed by systemic suppression of NK cells using a specific antibody, which resulted in significantly enhanced and

prolonged intratumoral viral titers.<sup>23</sup> We further demonstrated that suppression of chemotaxis of antiviral inflammatory cells could be achieved by genetic modification of the rVSV genome to express a heterologous vCKBP. In that study, we tested a rVSV vector encoding the secreted form of glycoprotein G from equine herpes virus-1 ( $gG_{EHV-1}$ ), which has demonstrated vCKBP activity and binds a broad range of chemokines with high affinity.<sup>25</sup> The  $gG_{EHV-1}$  protein blocks chemokine activity by preventing interactions with specific receptors and glycosaminoglycans, which are required for the correct presentation and function of chemokines. We showed that rVSV-gG treatment resulted in an inhibition of intratumoral NK and NKT cells, which in turn led to elevated VSV-mediated oncolysis, tumor response and substantial survival prolongation. Although the rVSV-gG vector proved to be a promising therapeutic agent for the treatment of multi-focal HCC, we faced concerns about the prospect of expressing a broad-range chemokine inhibitor, especially in light of the fact that our aim was to specifically inhibit NK cells. Therefore, we sought an alternate strategy in which we could specifically block the antiviral function of NK cells, while leaving all other aspects of the inflammatory response intact.

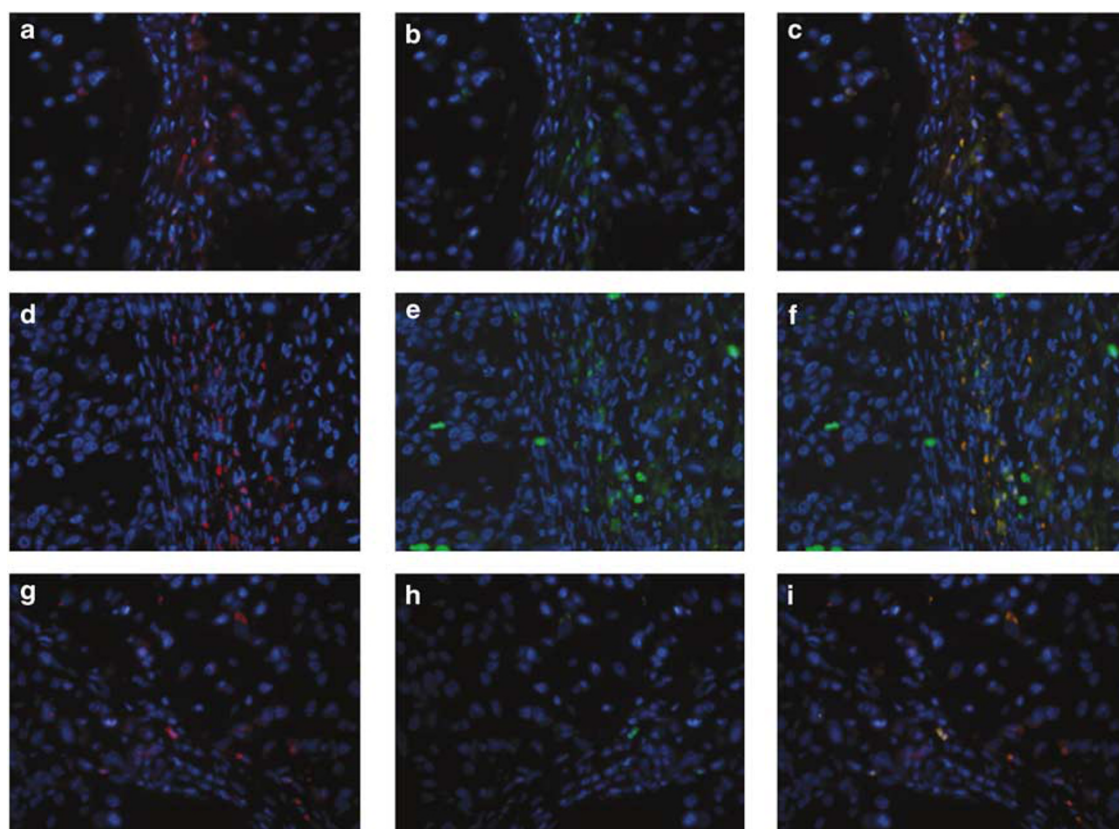


**Figure 6** Immunofluorescent staining of T and NK cells in tumors. Tumor-bearing Buffalo rats were infused through the hepatic artery with phosphate-buffered saline (PBS) (a–c), rVSV-F (frames d–f) or rVSV-UL141 (frames g–i) at  $1 \times 10^7$  p.f.u.  $ml^{-1}$  per rat. Samples were obtained at day 3 after virus infusion. Here, 5- $\mu m$  frozen sections were fixed with cold acetone and blocked with 4% goat serum, followed by staining with R-phycoerythrin (PE)-conjugated mouse anti-rat CD3 monoclonal antibody (a, d, g) and fluorescein isothiocyanate (FITC)-conjugated mouse anti-rat NKR-P1A (b, e, h). Merged pictures are shown in (c, f, i), respectively. Original magnification  $\times 40$ .

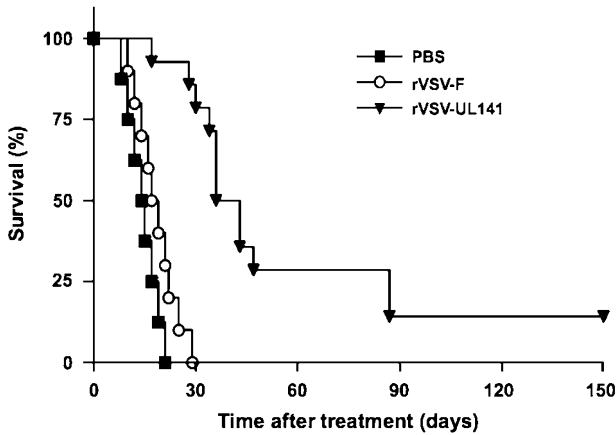


**Figure 7** Kaplan–Meier survival curve of multi-focal hepatocellular carcinoma (HCC)-bearing Buffalo rats after hepatic arterial infusion of phosphate-buffered saline (PBS) ( $n=8$ ), rVSV-F ( $n=10$ ) or rVSV-UL141 ( $n=14$ ) at  $1 \times 10^7$  p.f.u. ml<sup>-1</sup> per rat. Survival was monitored daily and the results were analyzed statistically by log-rank test ( $P<0.001$  for rVSV-UL141 versus rVSV-F).

UL141 is a viral gene product of HCMV. HCMV is a human herpesvirus, which causes persistent, lifelong infection, during which the host’s innate and adaptive immune responses work together to keep the virus in check.<sup>30–32</sup> In particular, NK cells are crucial in the control of cytomegalovirus infections; however, a key aspect of the capacity of HCMV to persist in the host is its ability to evade NK cell recognition.<sup>33–35</sup> In fact, at least six different HCMV genes encoding NK cell inhibitory function have been identified. One of these genes, UL141, modulates NK function by blocking cell surface expression of CD155,<sup>26</sup> which is a ligand for NK cell-activating receptors CD226 and CD96.<sup>36,37</sup> It was shown that expression of a transfected, secreted form of UL141 resulted in efficient protection of cells against killing by a wide range of human NK cell populations tested.<sup>26</sup>

To test the potential of UL141 for the purpose of VSV-mediated evasion of the inhibitory effects of NK cells, we created a recombinant vector, rVSV-UL141, in which the secreted form of UL141 was expressed as an additional transcription unit. This vector was then subjected to a series of *in vitro* analyses to fully characterize its features. To test the growth kinetics of the recombinant vector, we performed multi-cycle growth curves to rule out the possibility that expression of the transgene could inadvertently attenuate viral replication. At all time points tested, rVSV-UL141 demonstrated equivalent viral yields as compared to the control rVSV-F vector. Furthermore, the cell viability (MTT) assays revealed similar levels of cell killing in response to both vectors in the rat HCC cell line, McA-RH7777. Although there is no available antibody to UL141, and we were therefore unable to confirm or quantify the production of UL141 protein produced by the vector, we confirmed the function of UL141 in the recombinant vector, by performing *in vitro* migration assays. Although infection with the control vector, rVSV-F, induced the migration of NK cells, this

effect was significantly impeded in the presence of media conditioned by rVSV-UL141 infection. This indicates that expression of UL141 resulted in functional inhibition of NK cells, as predicted.

To define the *in vivo* implications of the genetically modified rVSV vector expressing UL141, in terms of its ability to evade the inhibitory function of NK cells and allow enhanced viral replication and cell killing, we tested the vector in our multi-focal HCC rat model. On day 3 after treatment by hepatic artery infusion, we confirmed that positive staining for VSV-G protein was indeed augmented within tumors of rats treated with rVSV-UL141 as compared with the control rVSV-F vector, and intratumoral virus titers increased by one-log. Furthermore, rVSV-UL141 treatment led to significantly enhanced tumor necrosis. Taken together, these results indicate that the modified vector results in enhanced replication and improved tumor response, as compared with the rVSV-F vector. Although rVSV-UL141 was not quite as effective in prolonging survival as our previously reported rVSV-gG vector, we reason that a slight compromise in efficacy is justified by a more controlled regulation of antiviral inflammation, which would minimize safety concerns. Furthermore, in addition to the potential clinical implications of this work, by creating a vector that specifically blocks the effects of NK and NKT cells, as opposed to the broad-range chemokine-binding function of the gG vector, we were able to elucidate the role of these cell types in oncolytic viral therapy.

To examine the mechanism whereby expression of UL141 resulted in substantially elevated intratumoral rVSV titers, we performed immunohistochemical staining of various immune cell types in tumor sections from animals treated with PBS, rVSV-UL141 or rVSV-F. As anticipated, NK cells seemed to be the major immune cell type recruited in response to rVSV-F infection. In contrast, rVSV-UL141 treatment resulted in a drastic reduction in NK cell accumulation to levels roughly equivalent to those observed in PBS-treated tumors. In addition, we noted a decrease in pan-T-positive cells within tumors treated with rVSV-UL141 as compared with rVSV-F. Subsequent immunofluorescence staining revealed that the pan-T-positive cells colocalized to NK marker-positive cells, indicating that these were in fact NKT cells. Finally, VSV-mediated expression of UL141 appeared to have no major impact on neutrophil or macrophage infiltration in HCC tumors.

NK cells are a major component of the innate cellular immune response, and are crucial in the early defense against invading pathogens.<sup>38,39</sup> NK cells are found primarily in the blood and spleen, as well as in non-lymphoid tissues such as liver, lung and peritoneal cavity.<sup>40,41</sup> These cells represent a distinct subset of the cytotoxic lymphocyte population, and act as a first line of defense against invading pathogens and viruses prior to the launch of the adaptive immune response.<sup>39,42,43</sup> On activation during viral infection, NK cells mediate the direct lysis of target cells by releasing cytotoxic granules containing lytic enzymes, or by binding to apoptosis-

inducing receptors on the target cell.<sup>33,44</sup> An *in vitro* study using HSV and vaccinia virus in human colon adenocarcinoma cells (Colo-205) revealed that NK cells preferentially lyse virus-infected cells at an early stage of infection, thereby preventing viral dissemination to neighboring cells.<sup>43</sup> These data support our hypothesis that the rapid recruitment of NK cells to VSV-infected tumor tissue impedes the viral spread and, in turn, the oncolytic potential of VSV therapy. This is also consistent with our observation that vector-mediated expression of UL141<sub>HCMV</sub>, a heterologous viral protein with known NK inhibitory function, resulted in enhanced VSV replication in the tumors.

By means of immunofluorescent analysis, a second type of inflammatory cells inhibited by rVSV-UL141 was identified as NKT cells. NKT cells represent a subset of NK cells, found within the T-cell population.<sup>44</sup> Although they represent only a small percentage of T cells found in the thymus and spleen, they constitute a significant proportion of those in the liver, accounting for approximately 25% of resident intrahepatic lymphocytes.<sup>45</sup> Although the mechanism and function of NKT cells in the inflammatory response are not completely understood, there is speculation that they may play a complementary role to NK cells in mediating early antiviral responses.<sup>44</sup> Although an inhibitory function of UL141<sub>HCMV</sub> on NKT cells has not been reported earlier, our results can be explained by the expression of CD226 on the surface of NKT cells. CD226 is an NK cell-activating receptor, ligand of which, CD155, is directly blocked by UL141. Therefore, an inhibitory effect on NKT cells, in addition to classical NK cells could be predicted. Furthermore, because viruses continuously evolve in such a way to promote their own survival within the infected host, it might be postulated that the viral genome of HCMV has selected mechanisms that evade the antiviral assault by NK and NKT cells to persist in immune-competent hosts.

Although the potent anti-NK and -NKT properties of UL141 made it a powerful candidate for exploitation within the context of improved oncolytic VSV therapy for HCC, the safety implications of such a strategy must be carefully considered. One could argue that, because endogenous expression of UL141 by HCMV contributes to the ability of the virus to cause lifelong infections in humans, rVSV expression of UL141 could result in a similar outcome. This possibility would be detrimental to the development of such a vector for future clinical application. To address this concern, we demonstrated earlier through comprehensive toxicity studies in immune-competent tumor-bearing rats, that our rVSV-gG vector introduced no additional toxicities as compared with the rVSV-F vector, despite the fact that gG<sub>EHV-1</sub> is known to be a broad-spectrum chemokine-binding protein, and effectively inhibited the chemotaxis of NK and NKT, and potentially other undefined cell types, to virus-infected lesions. Because the function of UL141<sub>HCMV</sub> is specific for NK and NKT cells, we predicted that rVSV-UL141 should be similar to rVSV-gG in its safety profile. Furthermore, throughout the long-term survival experiments conducted in the present study, the animals were carefully monitored for clinical signs of toxicity. rVSV-UL141 treatment

resulted in no significant weight loss, signs of dehydration, piloerection, limb paralysis or lethality. This absence of toxicity, despite evasion of key players in the antiviral inflammatory response, can be reconciled by the exquisite sensitivity of VSV to the type I interferon response in normal cells,<sup>44</sup> which is unaltered in the modified vector.

A final consideration of the current study involves the complexity of NK function in immune-competent hosts. Although we have discussed in detail the antiviral function of NK cells, it is important to also consider the role of NK cells in antitumor immunity. Interestingly, others have shown that NK cells can actually augment the tumoricidal effects of oncolytic herpes simplex virus, acting synergistically with the robust adoptive antitumor immune response launched in response to viral antigens expressed by tumor cells.<sup>21,46,47</sup> Even more striking, it has recently been reported that NK cells are required for the efficacy of VSV therapy in a melanoma model.<sup>48</sup> Here, it was proposed that the oncolytic potential of VSV is enhanced by antitumor immune responses. These contradictory results to our current study can be resolved by an understanding of the dual function of NK cells. On the one hand, it is well established that NK cells are potent inhibitors of viral replication, and it is this function that is inhibited by UL141. On the other hand, NK cells play a role in antitumor immunity, a feature that is enhanced by the presence of viral antigens within tumor cells. Although both strategies are scientifically sound, each approach contradicts the other. Although it would be quite interesting to compare both approaches side by side within the same tumor model, these studies are beyond the scope of the current investigation. Furthermore, to examine whether the impressive results obtained by rVSV-UL141 are limited to the treatment of HCC, or if they can also be applied to other cancers, it will be interesting to test this vector in other cancer models. These experiments are among our future plans.

In summary, we have presented a novel recombinant VSV vector, which exploits a specific NK and NKT cell inhibitor from HCMV. We have provided conclusive evidence that this modified vector demonstrates superior replication and oncolysis, resulting in significant prolongation of survival in a multi-focal HCC tumor model in rats. Moreover, this vector maintains the same safety profile as the wild-type vector. Thus, rVSV-UL141 has the potential for development into an effective and safe therapeutic agent for the treatment of HCC and possibly other types of cancer in the future. Furthermore, as antiviral inflammatory responses are universal obstacles limiting the potential of therapeutic viruses, the technology developed here is likely to be applicable in substantially enhancing the potency and efficacy of a wide spectrum of other oncolytic virus agents in cancer treatment as well.

#### Acknowledgements

We thank Dr Tian-gui Huang for helpful discussions, Dr Swan Thung for consultation on histological and

immunohistochemical analyses of tissue samples, and Mr Boxun Xie, Ms Yafang Wang and Ms Sonal Harbaran for excellent technical assistance. This study was supported, in part, by National Institutes of Health Grant CA100830 (SLCW), the German Research Aid (Max-Eder Research Program) (OE) and the Federal Ministry of Education and Research Grant 01GU0505 (OE).

## References

- Parkin DM, Sthernsward J, Muir CS. Estimates of the worldwide frequency of twelve major cancers. *Bull World Health Organ* 1984; **62**: 163–182.
- Murray CJ, Lopez AD. Evidence-based health policy—lessons from the Global Burden of Disease Study. *Science* 1996; **274**: 740–743.
- Parkin DM, Bray F, Ferlay J, Pisani P. Estimating the world cancer burden: Globocan 2000. *Int J Cancer* 2001; **94**: 153–156.
- El-Serag HB, Mason AC. Rising incidence of hepatocellular carcinoma in the United States. *N Engl J Med* 1999; **340**: 745–750.
- Dyer Z, Peltekian K, van Zanten SV. The changing epidemiology of hepatocellular carcinoma in Canada. *Aliment Pharmacol Ther* 2005; **22**: 17–22.
- Yeung YP, Lo CM, Liu CL, Wong BC, Fan ST, Wong J. Natural history of untreated nonsurgical hepatocellular carcinoma. *Am J Gastroenterol* 2005; **100**: 1995–2004.
- Cunningham S, Choti MA, Bellavance EC, Pawlik TM. Palliation of hepatic tumors. *Surg Oncol* 2007; **16**: 277–291.
- Rougier P, Mitry E, Barbare JC, Taieb J. Hepatocellular carcinoma (HCC): an update. *Semin Oncol* 2007; **34**: S12–S20.
- Kirn D, Martuza RL, Zwiebel J. Replication-selective virotherapy for cancer: biological principles, risk management, and future directions. *Nat Med* 2001; **7**: 781–787.
- Coffey MC, Strong JE, Forsyth PA, Lee PW. Reovirus therapy of tumors with activated Ras pathway. *Science* 1998; **282**: 1332–1334.
- Lorence RM, Katubig BB, Reichard KW, Reyes HM, Phuangsab A, Sassetti MD *et al*. Complete regression of human fibrosarcoma xenografts after local Newcastle disease virus therapy. *Cancer Res* 1994; **54**: 6017–6021.
- Peng KW, Ahmann GJ, Pham L, Greipp PR, Cattaneo R, Russell SJ. Systemic therapy of myeloma xenografts by an attenuated measles virus. *Blood* 2001; **98**: 2002–2007.
- Stojdl DF, Lichty B, Knowles S, Marius R, Atkins H, Sonenberg N *et al*. Exploiting tumor-specific defects in the interferon pathway with a previously unknown oncolytic virus. *Nat Med* 2000; **6**: 821–825.
- Letchworth GJ, Rodriguez LL, Del C, Barrera J. Vesicular stomatitis. *Vet J* 1999; **157**: 239–260.
- Rose JK, Whitt MA. Rhabdoviridae: the viruses and their replication. In: Knipe DM, Howley PM (eds). *Fields Virology*, 4th edn. Lippincott Williams & Wilkins: Philadelphia, 2001, pp 1221–1242.
- Ebert O, Shinozaki K, Huang TG, Savontaus MJ, Garcia-Sastre A, Woo SLC. Oncolytic vesicular stomatitis virus for treatment of orthotopic hepatocellular carcinoma in immune-competent rats. *Cancer Res* 2003; **63**: 611–613.
- Shinozaki K, Ebert O, Kournioti C, Tai YS, Woo SL. Oncolysis of multifocal hepatocellular carcinoma in the rat liver by hepatic artery infusion of vesicular stomatitis virus. *Mol Ther* 2004; **9**: 368–376.
- Ebert O, Shinozaki K, Kournioti C, Park MS, Garcia-Sastre A, Woo SL. Syncytia induction enhances the oncolytic potential of vesicular stomatitis virus in virotherapy for cancer. *Cancer Res* 2004; **64**: 3265–3270.
- Shinozaki K, Ebert O, Suriawinata A, Thung S, Woo S. Prophylactic alpha interferon treatment increases the therapeutic index of oncolytic vesicular stomatitis virus virotherapy for advanced hepatocellular carcinoma. *J Virol* 2005a; **79**: 13705–13713.
- Guidotti LG, Chisari FV. Noncytolytic control of viral infections by the innate and adaptive immune response. *Ann Rev Immunol* 2001; **19**: 65–91.
- Wakimoto H, Johnson PR, Knipe DM, Chioocca EA. Effects of innate immunity on herpes simplex virus and its ability to kill tumor cells. *Gene Therapy* 2003; **10**: 983–990.
- Wakimoto H, Fulci G, Tuminiski E, Chioocca EA. Altered expression of antiviral cytokine mRNAs associated with cyclophosphamide's enhancement of viral oncolysis. *Gene Therapy* 2004; **11**: 214–223.
- Altomonte J, Wu L, Chen L, Meseck M, Ebert O, Garcia-Sastre A *et al*. Exponential enhancement of oncolytic vesicular stomatitis virus potency by vector-mediated suppression of inflammatory responses *in vivo*. *Mol Ther* 2008; **16**: 146–153.
- Alcami A. Viral mimicry of cytokines, chemokines, and their receptors. *Nat Immunol* 2003; **3**: 36–50.
- Bryant NA, Davis-Poynter N, Vanderplasschen A, Alcami A. Glycoprotein G isoforms from some alphaherpesviruses function as broad-spectrum chemokine binding proteins. *EMBO J* 2003; **22**: 833–846.
- Tomasec P, Wang E, Davison A, Vojtesek B, Armstrong M, Griffin C *et al*. Downregulation of natural killer cell-activating ligand CD155 by human cytomegalovirus UL141. *Nat Immunol* 2005; **6**: 181–188.
- Lawson ND, Stillman EA, Whitt MA, Rose JK. Recombinant vesicular stomatitis viruses from DNA. *Proc Natl Acad Sci USA* 1995; **92**: 4477–4481.
- Whelan SP, Ball LA, Barr JN, Wertz GT. Efficient recovery of infectious vesicular stomatitis virus entirely from cDNA clones. *Proc Natl Acad Sci USA* 1995; **92**: 8388–8392.
- Shinozaki K, Ebert O, Woo SL. Eradication of advanced hepatocellular carcinoma in rats via repeated hepatic arterial infusions of recombinant VSV. *Hepatology* 2005; **41**: 196–203.
- Guma M, Angulo A, Lopez-Botet M. NK cell receptors involved in the response to human cytomegalovirus infection. *Curr Top Microbiol Immunol* 2006; **298**: 207–223.
- Lin A, Xu H, Yan W. Modulation of HLA expression in human cytomegalovirus immune evasion. *Cell Mol Immunol* 2007; **4**: 91–98.
- Lopez-Botet M, Llano M, Ortega M. Human cytomegalovirus and natural killer-mediated surveillance of HLA class I expression: a paradigm of host-pathogen adaptation. *Immunol Rev* 2001; **181**: 193–202.
- Orange JS, Fassett MS, Koopman LA, Boyson JE, Strominger JL. Viral evasion of natural killer cells. *Nat Immunol* 2002; **3**: 1006–1012.
- Rajagopalan S, Long EO. Viral evasion of NK-cell activation. *Trends Immunol* 2005; **26**: 403–405.
- Wilkinson G, Tomasec P, Stanton RJ, Armstrong M, Prod'homme V, Aichele R *et al*. Modulation of natural killer cells by human cytomegalovirus. *J Clin Virol* 2008; **41**: 206–212.
- Bottino C, Castriconi R, Pende D, Rivera P, Nanni M, Carnemolla B *et al*. Identification of PVR (CD155) and

- Nectin-2 (CD112) as cell surface ligands for the human DNAM-1 (CD226) activating molecule. *J Exp Med* 2003; **198**: 557–567.
- 37 Fuchs A, Cella M, Giurisato E, Shaw AS, Colonna M. Cutting edge: CD96 (tactile) promotes NK cell-target cell adhesion by interacting with the poliovirus receptor (CD155). *J Immunol* 2004; **172**: 3994–3998.
- 38 Biron CA, Nguyen KB, Pien GC, Cousens LP, Salazar-Mather TP. Natural killer cells in antiviral defense: function and regulation by innate cytokines. *Ann Rev Immunol* 1999; **17**: 189–220.
- 39 Welsh RM. Regulation of virus infections by natural killer cells. *Nat Immun Cell Growth Reg* 1986; **5**: 169–199.
- 40 Trinchieri G. Biology of natural killer cells. *Adv Immunol* 1989; **47**: 187.
- 41 Cerwenka A, Lanier LL. Natural killer cells, viruses and cancer. *Nat Rev Immunol* 2001; **1**: 41–49.
- 42 Brutkiewicz RR, Welsh RM. Major histocompatibility complex class I antigens and the control of viral infections by natural killer cells. *J Virol* 1995; **69**: 3967–3971.
- 43 Baraz L, Khazanov E, Condiotti R, Kotler M, Nagler A. Natural killer (NK) cells prevent virus production in cell culture. *Bone Marrow Transplant* 1999; **24**: 179–189.
- 44 Biron CA, Brossay L. NK cells and NKT cells in innate defense against viral infections. *Curr Opin Immunol* 2001; **13**: 458–464.
- 45 Eberl G, Lees R, Smiley ST, Taniguchi M, Grusby MJ, MacDonald HR. Tissue-specific segregation of CD1d-dependent and CD1d-independent NK T-cells. *J Immunol* 1999; **162**: 6410–6419.
- 46 Todo T, Martuza RL, Rabkin SD, Johnson PA. Oncolytic herpes simplex virus vector with enhanced MHC class I presentation and tumor cell killing. *Proc Natl Acad Sci USA* 2001; **98**: 6396–6401.
- 47 Thomas D, Fraser NW. HSV-1 therapy of primary tumors reduces the number of metastases in an immune-competent model of metastatic breast cancer. *Mol Ther* 2003; **8**: 543–551.
- 48 Diaz R, Galivo F, Kottke T, Wongthida P, Qiao J, Thompson J et al. Oncolytic immunovirotherapy for melanoma using vesicular stomatitis virus. *Cancer Res* 2007; **67**: 2840–2848.